Signal-to-noise ratios of teleseismic receiver functions and effectiveness of stacking for their enhancement

Igor B. Morozov and Kenneth G. Dueker

Department of Geology and Geophysics, University of Wyoming, Laramie, WY 82071-3006

Submitted to *JGR*

Address for correspondence:

Igor B. Morozov
Department of Geology and Geophysics
University of Wyoming
Laramie, WY 82071-3006
Tel. 307 766 4905
Fax 307 766 6679
morozov@uwyo.edu

ABSTRACT

We present a method for quantitative measurement of spatially variable signal-to-noise ratios in multichannel teleseismic receiver function (RF) images. The method uses a modification of 3D pre-stack depth migration in which the records are first mapped to depth using the *PdS* mode conversion kinematics, so that all the converted phases become horizontally aligned in depth domain. After this, the dataset is bootstrapped multiple times and the signal and incoherent noise amplitudes are estimated from stacking statistics. For ten locations along the two subarrays of the Continental Dynamics of Rocky Mountains Project (CD-ROM), after a limited RF editing, we find the signal-to-noise ratios (S/N) to vary from 0.1 to 0.25. These values argue strongly in favor of sampling redundancy achieved in array recording and multi-channel RF processing. For a typical present-day array recording such as the CD-ROM, conventional pre-stack depth migration results in RF sections with S/N ranging between about 1.5-4, with significant spatial variability in S/N. In order to further reduce noise contamination of RF images, denser and longer deployments or additional signal enhancement techniques are advisable. Due of its ability to provide direct assessment of image quality in 3D, including its dependence on the frequency band and data coverage, our method could be also used for real-time array tuning and image focusing required for large-aperture, dense, migrating arrays such as proposed for the USARRAY program.

INTRODUCTION

Teleseismic receiver functions (RF) are broadly used for imaging the Moho and mantle discontinuities [e.g., *Vinnik*, 1977; *Ammon* et al., 1990; *Shearer*, 1991; *Bostock*, 1996; *Dueker and Sheehan*, 1998; *Shen* et al., 1998; *Chevrot* et al, 1999; *Gurrola and Minster,* 2000; *Lewis* et al., 2001]. With the advent of dense portable PASSCAL broad-band arrays [*Dueker and Sheehan*, 1998; *Neal and Pavlis*, 1999; Bostock and Rondenay,1999] the volumes of RF datasets have increased dramatically, and so did the claim for detailed RF imaging of the upper mantle between the surface and transition zone. Several source- and receiver-array imaging techniques were developed, such as common conversion point stacking [*Dueker and Sheehan*, 1998], velocity spectrum stacking [*Gurrola* et al., 1994; *Shen* et al., 1998], t-p record interpolation [*Neal and Pavlis*, 1999], and pre-stack depth migration [e.g., *Bostock and Rondenay*, 1999; *Sheehan* et al., 2000; *Poppeliers and Pavlis*, 2002]. All of these techniques ultimately rely on some kind of record summation (stacking) for signal enhancement; however, no quantitative measurements of noise in RF stacks have been performed so far.

Significant level of scattering noise in RF records has been recognized, particularly at higher frequencies [e.g., *Abers*, 1998], and stacking techniques for noise suppression are broadly used. However, a number of critical questions still remain to be answered quantitatively before the problem of noise in RF images is resolved. How could the noise level in RF records be determined? How many records need to be stacked for a meaningful interpretation? How efficient is stacking and is it the optimal processing for the attenuation of noise? Finally, and most importantly, what is the level of noise remaining in the resulting images?

The purpose of this note is to present a simple estimate of signal-to-noise ratio (S/N) in a RF image and to discuss the effectiveness of stacking for its enhancement. Our definition of S/N

ratio focuses specifically on assessment of image quality resulting from a stacking-based imaging technique and differs from the measures of recording channel noise usually employed [e.g., *Poppeliers and Pavlis*, 2002b]. In the discussion below, S/N measures the proportion of coherent signals from *PdS* conversions as opposed to multiples and other phases inconsistent with *PdS* kinematics, and also to incoherent noise.   The key requirement to the imaging technique is multiplicity of data sampling that allows identification of such a coherent component. As such a multichannel imaging approach, we use a broad group of methods represented by 3D pre-stack depth migration; most of the existing multichannel imaging methods either belong to this group or can be easily rendered in its general form of time-to-depth mapping and subsequent record summation.

Using the data from the teleseismic CD-ROM experiment [*Dueker et al.* 2001], we demonstrate that in this data set, apparently representing a "typical" present-day linear broadband deployment, the noise component is not dominant but may be still significant in the resulting RF images. It appears that in order to improve consistency of imaging, we need to employ signal processing techniques that are more effective than stacking in noise suppression. Furthermore, since the RF image S/N ratios vary laterally and with target depth and are relatively easy to measure, monitoring these ratios during data acquisition could be used for real-time array adjustment and targeting during extended periods of deployment.

SIGNAL-TO-NOISE RATIOS IN RECEIVER FUNCTION DATA

Signal enhancement using straight (unweighted) stacking can be described using the following well-known simplified paradigm. Multiple recordings are assumed to have the same amplitude of "signal", $s(t)$, and the same noise power, $n^2(t)$, in all the channels. In contrast, the noise components, $n_i(t)$ and $n_j(t)$ are assumed to be uncorrelated between the different records:

$<n_i(t)n_j(t)>=0$ and with the signal: $<n_i(t)s(t)>=0$ (i and j are the numbers of the records). If we form a stack:

$$S(t) = \sum_{i=i}^{N}(s(t)+n_i(t)) = Ns(t) + \sum_{i=i}^{N}n_i(t),$$

its power can therefore be expressed as:

$$\left\langle S^2(t)\right\rangle = N^2\left\langle s^2(t)\right\rangle + \sum_{i=i}^{N}\left\langle n_i^2(t)\right\rangle = N^2\left\langle s^2(t)\right\rangle + N\left\langle n_i^2(t)\right\rangle. \qquad (1)$$

With increasing number of records N, the signal power in the stack increased as N^2 while the noise power increases linearly resulting in a $\sqrt{N}$ increase in the amplitude signal-to-noise ratio. Note that the noise power in the stack does not decrease as it is sometimes assumed. Rewriting relation (1) in terms of the mean stack power:

$$\frac{\left\langle S^2(t)\right\rangle}{N} = N\left\langle s^2(t)\right\rangle + \left\langle n_i^2(t)\right\rangle, \qquad (2)$$

we obtain a simple estimator of the signal-to-nose ratio, both in the original data and in the stack. In the presence of coherent signal, the mean stack power (2) should exhibit a linear dependence on N. With a sufficiently large number of records available for stacking, this behavior can be tested by random resampling (bootstrapping) the dataset and fitting a linear regression for $<S^2>/N$ as a function of N.

Before the mean stack power (2) can be computed from RF data, however, travel time moveouts due to the differences in ray parameters, backazimuths, and relative station positions must be removed, so that the coherent, $s(t)$, component of the records can be regarded as identical in all the channels. A very general way for doing such normalization is to perform travel-time to depth mapping of the records at some imaging point, as it is commonly done in pre-stack depth migration (depending on the migration scheme employed, this step can also include amplitude

corrections [cf. *Bostock and Rondenay,* 1999]). After such mapping, the records are converted to depth, $s(t) \rightarrow s(z)$, forming an equivalent of the Common Image Gather (CIG) [e.g., *Al-Yahya*, 1989]. Within a CIG, all the true *PDS* mode conversions become horizontally aligned, thereby satisfying model (1). Note that such horizontal alignment is achieved regardless of the underlying mantle structure, provided the background velocity model correctly describes wave kinematics in the region of interest [*Al-Yahya*, 1989]. Any other energy inconsistent with the *PdS* conversion kinematics is misaligned in the CIG and is treated as noise.

We apply the above technique to RF data from a broadband array of the Continental Dynamics of the Rocky Mountains (CD-ROM) experiment acquired from June 1999 to June 2000. The two CD-ROM deployments consisted of 21 stations in each of the two lines, spaced at about 10-12 km (Figure 1). These arrays are among the relatively large and dense PASSCAL deployments operated recently and provide good datasets for detailed analysis of the upper mantle; they also could arguably considered "typical" linear arrays for our S/N study. For our measurements, we migrate all the records into each of the five selected points in each subarrays (gray dots in Figure 1), using the IASP91 velocity model. Although this velocity model is 1D, the ray kinematics is accurate in a 3D sense and takes into account the actual locations of the stations, ray parameters, and backazimuths.

About 1800 RFs were obtained using the standard frequency-domain deconvolution technique regularized using "water-level" of 1% [*Dueker and Sheehan*, 1998], and filtered using a zero-phase band pass filter between 0.3 and 2.0 Hz with one octave filter roll-off at both ends. This frequency band is considered a high S/N pass band for CD-ROM dataset [*Dueker et al.*, 2001]. For S/N measurements, only the records from the stations within 30-km distance from the imaging points were included in the analysis since these stations were considered the best

contributors to the image above the depth of ~100 km.   By repeated bootstrapping the migrated

RFs, we produced 3000 subsets of N records, where N was uniformly distributed between 0 and

120-270, depending on the imaging point. Finally, we stacked the remaining subsets, measured

the resulting stack power within two depth windows (Figure 2), and created scatter diagrams

(Figure 3).

The distributions of $<S^2>/N$ in Figure 3 show clear linear trends indicating the presence of

coherent signal in the data. By fitting straight lines to these distributions, we estimate the signal

power from the slopes of these lines, and noise power from their intersections with the axis $N=0$.

However, extrapolation of the $<S^2>/N$ dependence to low values of N may be relatively inaccurate

because of a trade-off with the slope of the regression, and a more reliable estimate of the noise

power can be derived from the widths of the distributions of $<S^2>/N$. Specifically, for our model

(1), the variance of mean stack power is:

$$\frac{\left\langle \left(S^2(t) - \left\langle S^2(t) \right\rangle \right)^2 \right\rangle}{N^2} = \left\langle n^2(t) \right\rangle \left[4\left\langle s^2(t) \right\rangle + \left\langle n^2(t) \right\rangle \left(1 - \frac{1}{N} \right)^2 \right] \approx \left\langle n^2(t) \right\rangle^2$$

when $<s^2> \ll <n^2>$, as indeed is often the case with RF data . This variance is independent of N

and can be estimated directly from the scatter diagrams, as about half-width of the distributions of

$<S^2>/N$ in vertical direction (Figure 3).

The resulting values of $<s^2>$ and $<n^2>$ suggest S/N values that are about 0.1-0.25 for the

Moho and mantle between 60-80 km depth respectively, and exhibit significant spatial variability

(Figure 4). The levels of S/N in the final migrated image vary by a factor of 2 within 30-60 km

distances; at a more regional scale, similar variations are indicated by the mantle S/N under the

northern subarray being consistently lower that of the Moho, whereas for the southern subarray

these levels are about the same (Figure 4b). Such moderate S/N values and their spatial variability

emphasize the importance of combining multiple recordings to enhance the resulting image, and also of monitoring S/N attributes for selection of imaging techniques, interpretation, and also potentially for array design in the future.

DISCUSSION AND CONCLUSIONS

With S/N ratios ranging between 0.1-0.25 (Figure 4), stacking of 16 to 100 records is required in order to bring the coherent signal to the level of noise, and twice as many are probably needed to ensure prevalence of PdS mode conversions in the resulting image. Such RF density is attained yet is close to the limit of data redundancy of the CD-ROM data set, where we estimate the S/N in the final stack ranging between 1.5 and 4, with some outliers dropping below this level (Figure 4). Therefore, assuming that signal amplitude consistently exceeding the incoherent noise by a factor of about 3 is desirable for robust imaging, we suggest that still denser and longer deployments are required.

Our technique of spatially variant depth-domain S/N estimation provides a direct test of the performance of pre-stack depth migration and stacking as the primary method for signal enhancement. As our results above suggest, with the existing data sets, stacking may result in images that are only moderately above the level of noise. It appears that because of the high level of random noise, conventional (summation-based) pre-stack depth migration is also likely to suffer from noise contamination with the present-day data sets. One way to overcome these shortcomings is in using still denser arrays and replacing stacking with more robust signal detection methods, such as median or coherency filtering in depth domain. Adaptive "dip filtering" in depth domain could also attenuate the coherent, source-induced noise and filtering artifacts that may be difficult to distinguish from PdS conversions because of the limited recording aperture. An alternative approach (also broadly used) is based on careful selection of RFs for

imaging; however, excessive record editing could be prone to subjectivity and would also reduce data redundancy necessary for consistent imaging and defeat any possibilities for quality control.

The above approach allows us to investigate the dependence of the signal-to-nose ratio on the location within the image, on the subset of data used, as well on the frequency band. Overall, the method provides a direct assessment of RF image quality in 3D. For large-aperture, dense arrays such as proposed for the USARRAY program, this method could readily provide maps of image quality attributes, such as the S/N ratios and CIG sampling. As our results suggest, this quality may vary significantly across short distances. With continuous monitoring of the image during migration of the array, such attributes could conceivably be used for real-time array tuning and RF image focusing.

ACKNOWLEDGEMENTS

REFERENCES

Abers, G. A., Array measurements of phase used in receiver function calculations: Importance of scattering, Bull. Seism. Soc. Am., 88, 313-318, 1998.

Al-Yahya, K., Velocity analysis by iterative profile migration, Geophysics, 54, 718-729, 1989.

Ammon, C. J., G. E. Randall, and G. Zandt, On the nonuniqueness of receiver function inversions, J. Geophys. Res., 95, 15,303-15,318, 1990.

Bostock, M. G., and S. Rondenay, Migration of scattered teleseismic body waves, Ps, Geophys. *J. Int*., 137, 732-746, 1999.

Chevrot, S., L. Vinnik, and J. P. Mintagner, Global-scale analysis of the mantle *Ps* phases, *J. Geophys. Res., 104*, 20,203-20,219, 1999.

Dueker, K, H. Yuan, and B. Zurek, Thick Structured Proterozoic Lithosphere of the Rocky Mountain Region, GSA Today, 4/12, 3-9, 2001.

Dueker, K. G., and A. F. Sheehan, Mantle discontinuity structure beneath the Colorado Rocky Mountains and High Plains, *J. Geophys. Res., 103*, 7153-7169, 1998.

Gurrola, H., and J. B. Minster, Evidence for local variations in the depth to the 410-km discontinuity beneath Albuquerque, New Mexico, *J. Geophys. Res., 105*, 10,847-10,856, 2000.

Gurrola, H., J. B. Minster, and T. Owens, The use of velocity spectrum for stacking receiver functions and imaging upper mantle discontinuities , *Geophys. J. In., 117*, 427-440, 1994.

Lewis, J. L., S. M. Day, H. Magistrale, R. Castro, L. Astiz, C. Rebollar, J. Eakins, F. L Vernon, and J. N. Brune, Crustal thickness of the Peninsular Ranges and Gulf Extensional Province in the Californias, J. Geophys. Res., 106, 13,599-13,611, 2001.

Morozov, I. B. and A. Levander, Depth image focusing in travel-time map based wide-angle migration, Geophysics, in press.

Morozov, I. B., and Smithson, S. B., A new system for multicomponent seismic processing, Computers & Geosciences, 23, 689-696, 1997.

Neal, S. L., and G. L. Pavlis, Imaging *P*-to-*S* conversions with multichannel receiver functions, Geophys. Res. Lett., 26, 2581-2584, 1999.

Poppeliers, C. and G. L. Pavlis, Three-dimensional, prestack, planewave migration of teleseismic P-to-S converted phases I: Theory, J. Geophys. Res., in review, 2002a.

Poppeliers, C., and G. L. Pavlis, Three-dimensional, prestack, planewave migration of teleseismic P-to-S converted phases 2: Stacking multiple events, *J. Geophys. Res.*, in review, 2002b.

Sheehan, A. F., Shearer, P., Gilbert, H. J., and Dueker, K. G., 2000. Seismic migration processing of P-SV converted phases for mantle discontinuity structure beneath the Snake River Plain, western United States, *J. Geophys. Res., 105*, 19,055-19,065.

Shen, Y., S. C. Solomon, I. T. Byarnason, and C. J. Wolfe, Seismic evidence for a lower-mantle origin of the Iceland Plume, *Nature, 395*, 62-65, 1998.

FIGURES
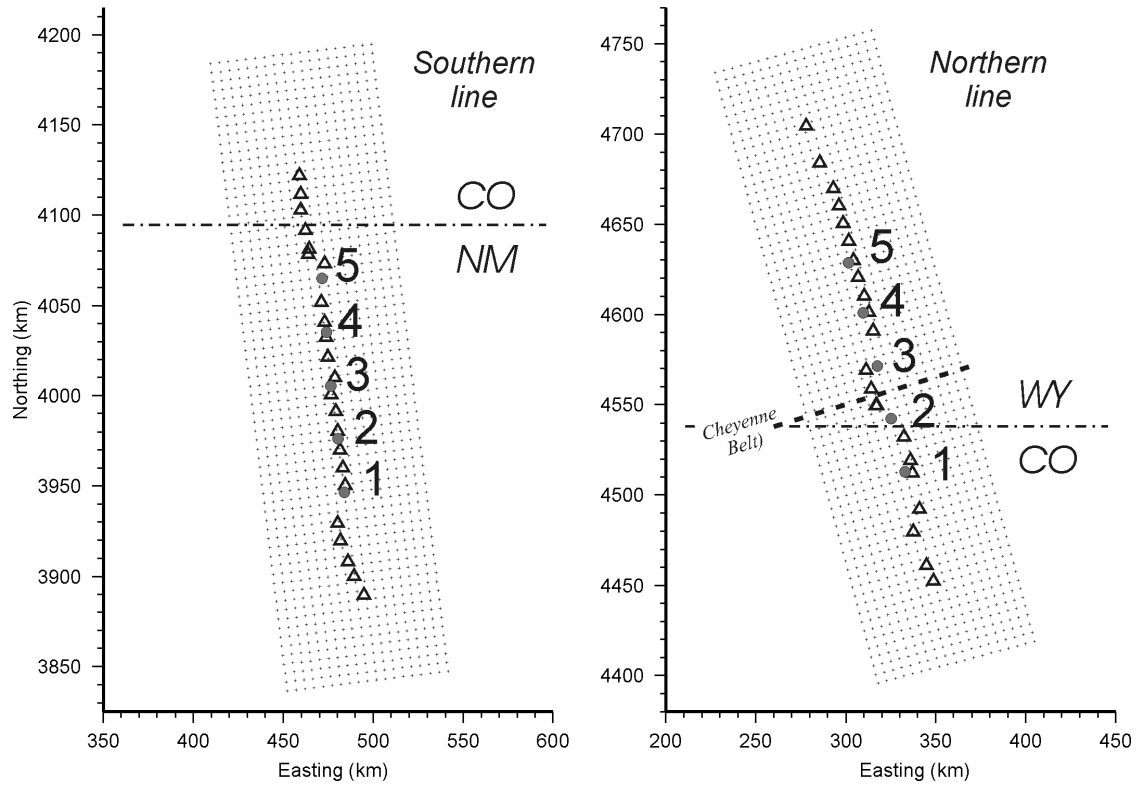
Figure 1. The southern and northern parts of the CD-ROM array. The approximate location of the Cheyenne Belt is shown with a thick dashed line. The rectangular 3D imaging grid is also shown. Five nodes along the axis of each grid are used in our S/N estimation (highlighted in gray and labeled 1-5. Coordinates are UTM, in kilometers.
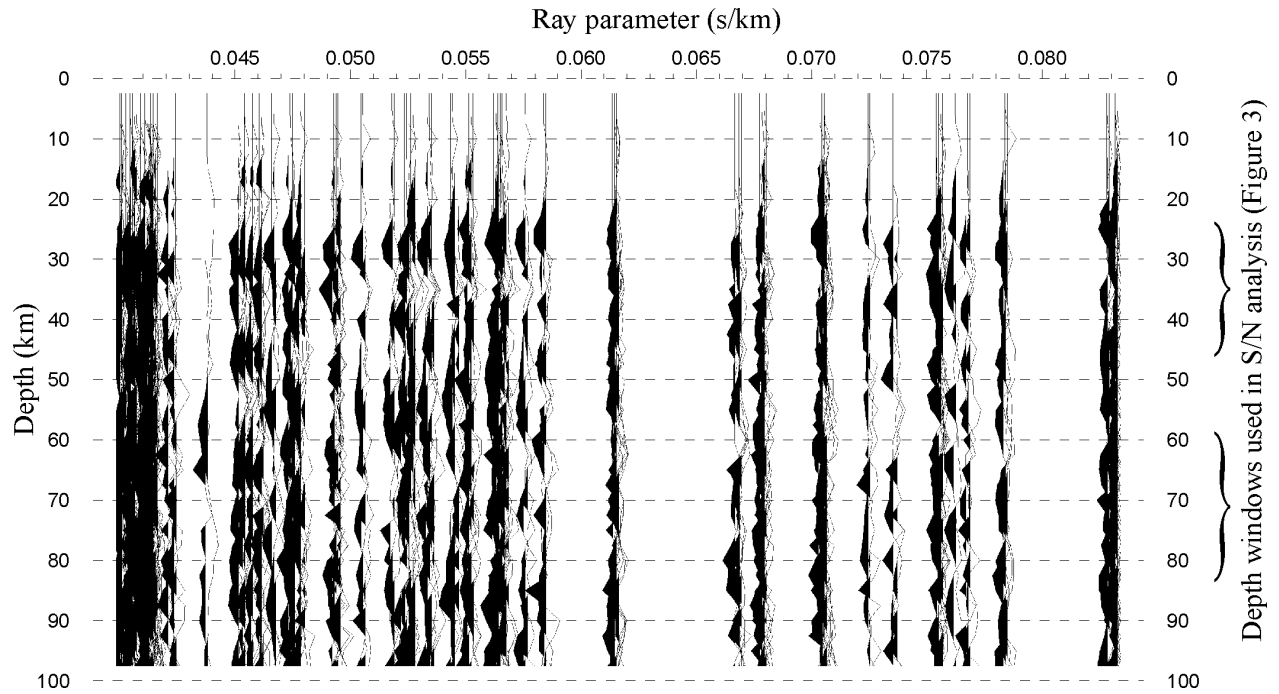
Figure 2. Common image gather (CIG) for the center of the southern imaging grid (large gray dot labeled 3 in Figure 1, left). A stack of these records would constitute the traditional pre-stack depth migrated image at this point. To illustrate their actual variability, the records are not binned, with multiple records plotted at the same values of ray parameter.

Northern CD-ROM line
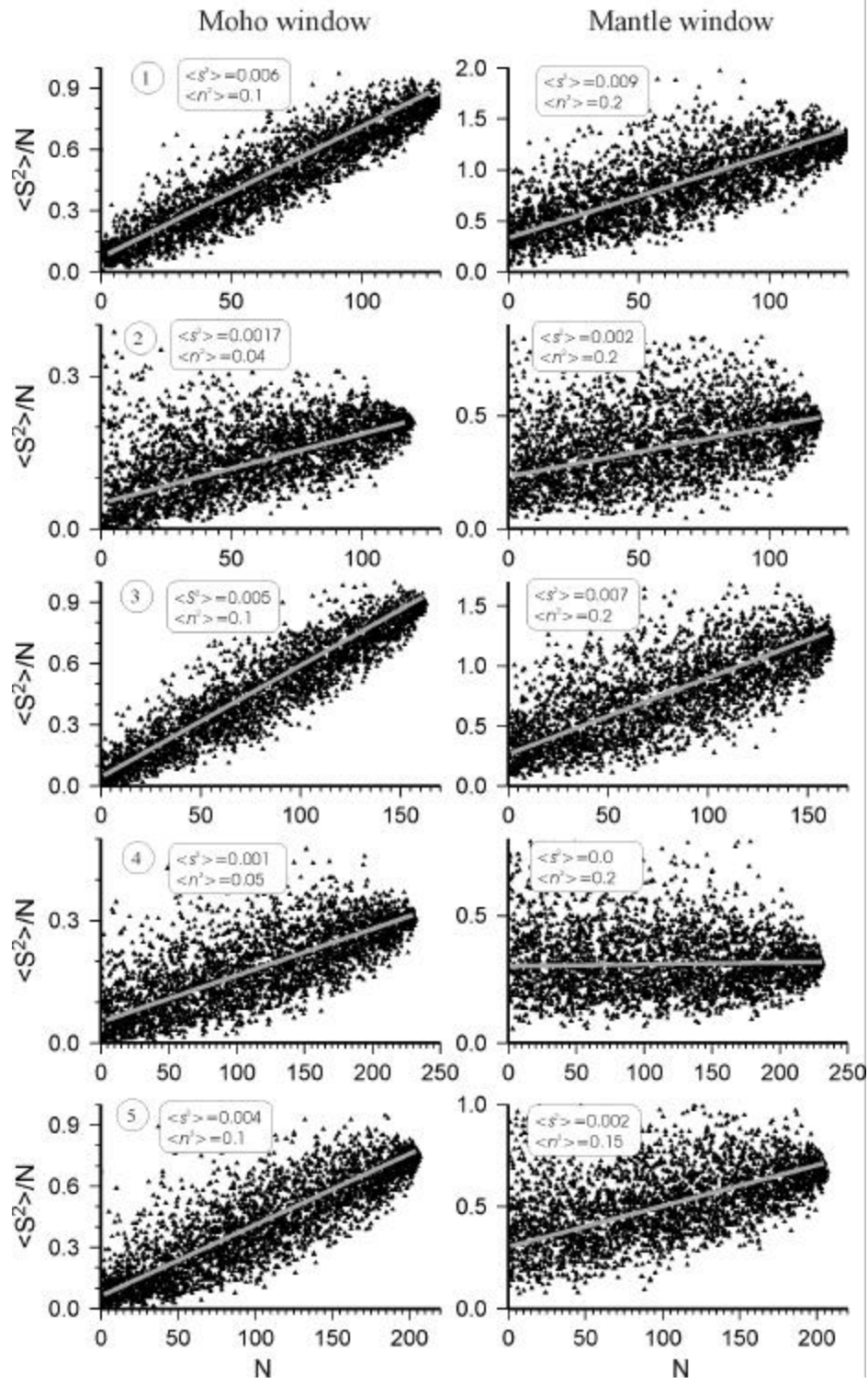
Figure 3. Dependence of the mean stack power (2) on the number of stacked depth-converted records within two depth windows (Figure 2) for the Moho *PDS* conversion and for a window between 70-100 km depth, measured for five imaging points (A through E) along the axis of each of the grid (Figure 1). The slopes of the axes of these distributions (gray dashed lines) provide estimates of mean signal power, $<s^2>$, and their widths correspond to noise power, $<n^2>$ (labeled). The units of RF amplitudes are relative.

Southern CD-ROM line

Moho window   Mantle window
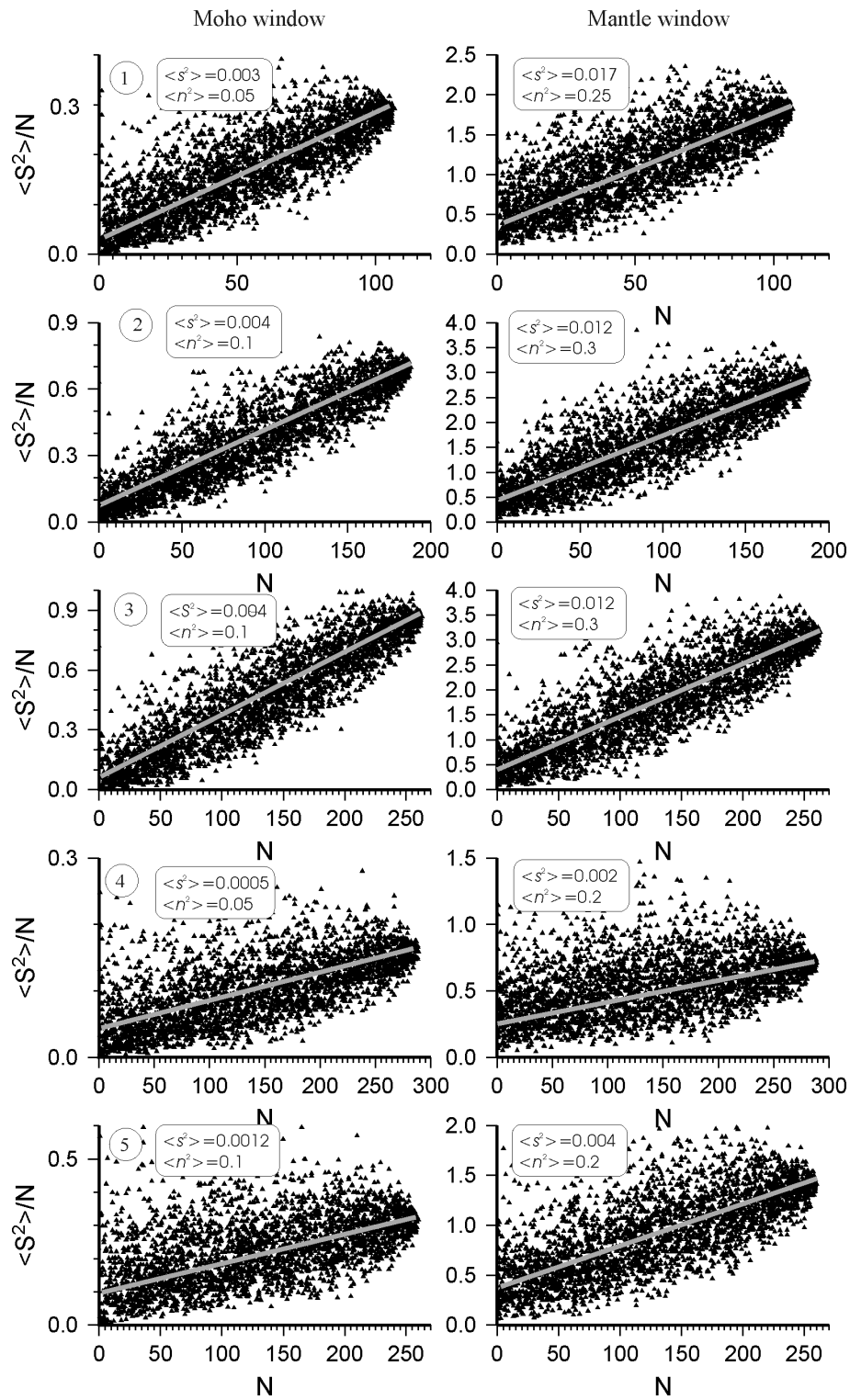
Figure 3, continued.
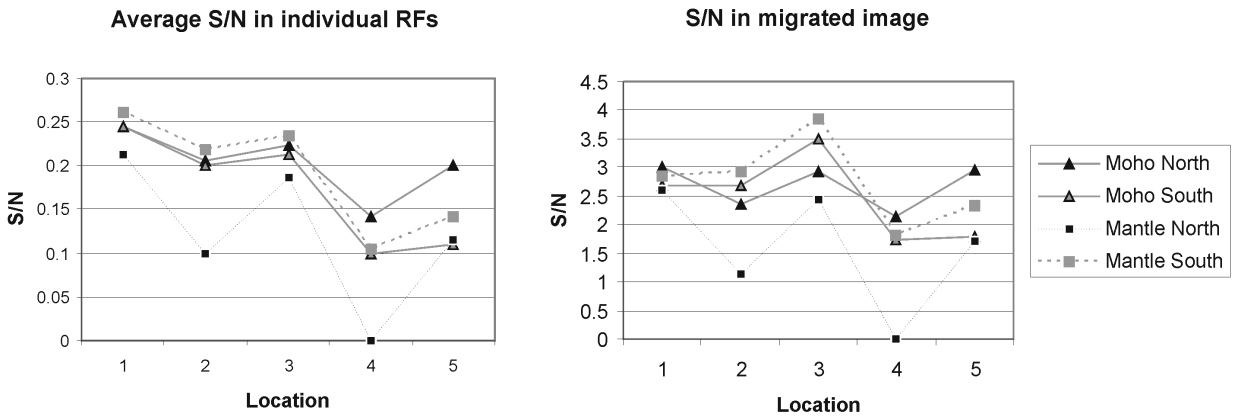
Figure 4. Amplitude S/N ratios determined from the signal and noise estimates in Figure 3. Note the variability of the values. Apart from two outliers with S/N≈0, the values are in the range 0.1-0.23, with somewhat higher values for the Moho.